Rangeland Ecology & Management 69 (2016) 84–94

Contents lists available at ScienceDirect

Rangeland Ecology & Management

journal homepage: http://www.elsevier.com/locate/rama

Grassland Carbon Sequestration Ability in China: A New Perspective from Terrestrial Aridity Zones☆

Yizhao Chen [a], Shaojie Mu [b], Zhengguo Sun [c], Chengcheng Gang [a], Jianlong Li [d,*], José Padarian [e], Pavel Groisman [f], Jingming Chen [g], Siwei Li [h]

[a] Associate Researcher, School of Life Science, Nanjing University, the People's Republic of (PR) China
[b] Researcher, Nanjing Institute of Environmental Sciences, Ministry of Protection, Nanjing, PR China
[c] Associate Professor, College of Animal Science and Technology, Nanjing Agriculture University, Nanjing, PR China
[d] Professor, School of Life Science, Nanjing University, the People's Republic of (PR) China
[e] Lecturer, Faculty of Agriculture and Environment, The University of Sydney, Sydney, Australia
[f] Professor, National Oceanic and Atmospheric Administration National Climatic Data Center, Asheville, North Carolina, NC 28801, USA
[g] Professor, Department of Geography, University of Toronto, Toronto, ON, Canada
[h] Postgraduate, School of Computer Science and Engineering, Nanjing University of Science and Technology, Nanjing, PR China

ARTICLE INFO

Article history:
Received 10 January 2015
Received in revised form 14 September 2015
Accepted 28 September 2015

Keywords:
aridity index
Chinese grassland
terrestrial biogeochemical modeling
terrestrial carbon cycle
water budget condition

ABSTRACT

Current climate change (e.g., temperature and precipitation variations) profoundly influences terrestrial vegetation growth and production, ecosystem respiration, and nutrient circulation. Grasslands are sensitive to climate change, and the carbon sequestration ability is closely related to water availability. However, how the terrestrial water budget influences regional carbon sequestration by the grassland ecosystem is still unclear. In this study, we modified a terrestrial biogeochemical model to investigate net ecosystem productivity (NEP) of Chinese grasslands under different aridity index (AI) levels from 1982 to 2008. The results showed that Chinese grasslands acted as a carbon sink of 33.7 TgC. yr^{-1}, with a clear decrease in the spatial distribution from the humid end (near-forest) to the arid end (near-desert). During these 27 years, gross primary productivity (GPP) and net primary productivity (NPP) significantly increased with regional warming over the entire range of the AI, but no significant tendency was found for NEP. Meanwhile, only NPP in the arid zone (AR) and the semiarid zone (SAR) were significantly correlated with mean annual precipitation (MAP), and no significant correlation was found between heterotrophic respiration (R_h) and MAP; NPP and R_h were both positively correlated with mean annual temperature (MAT) in all AI zones except for NPP in AR; no significant correlation between NEP and MAP or MAT was found. These results revealed that the grasslands with different AI levels keep different response patterns to temperature and precipitation variations. On the basis of these results, we predicted that the gap of carbon sequestration ability between humid and arid grassland will expand. The total carbon sink in Chinese grasslands will continue to fluctuate, but there is a danger that it might shrink in the future because of a combination of climatic and human factors, although CO_2 fertilization and N deposition might partly mitigate this reduction.

Introduction

According to the latest Intergovernmental Panel on Climate Change report (2013), global surface temperature increased by 0.85°C from 1880 to 2012 and will continue to rise by approximately 0.3—4.8°C in 2081–2100 compared with the temperature for 1986–2005. Given this situation, the global terrestrial carbon and hydrological cycles are experiencing and will continue to experience significant changes (Calzadilla et al. 2013; Gosling and Arnell 2013). Furthermore, because of the tight interactions between these two cycles, they will strongly affect each other as well (Falkowski et al. 2000; Porporato et al. 2003).

Grasslands cover approximately 44% of the total terrestrial area in China and comprise 13% of the world's total grasslands (Ni 2002, 2004a; Scurlock and Hall 1998). Grasslands are among the most important terrestrial carbon pools in China, storing approximately 3.06 Pg of vegetation carbon and 41.03 Pg of soil carbon (Ni 2002). The Chinese grasslands ecosystem is greatly affected by human activity via land use and cover change, direct graze, and mowing, so it is also

☆ Research was funded by APN Global Change Fund Project (ARCP2013-16NMY-Li), the National Natural Science Foundation of China (41271361); The Key Project of Chinese National Programs for Fundamental Research and Development (973 Program, 2010CB950702); the National High Technology Project (863 Plan, No. 2007AA10Z231); and the Public Sector Linkage Program supported by Australian Agency for International Development (64828).
* Correspondence: Jianlong Li, School of Life Science, Nanjing University, Hankou Road 22, Nanjing 210093, PR China.
E-mail address: Jianlongli@gmail.com (J. Li).

http://dx.doi.org/10.1016/j.rama.2015.09.003
1550-7424/

closely related to national agriculture and the animal husbandry system (Cao et al. 2011; Duan et al. 2011; Wang et al. 2011).

Grassland ecosystems are sensitive and vulnerable to global change (Fang et al. 2003; Ni 2003, 2004b; Piao et al. 2006c; Scurlock and Hall 1998). The impacts of CO_2 concentration, temperature, and precipitation variability can significantly affect the grassland carbon and water budget (Bai et al. 2010; Mitchell and Csillag 2001; Schimmelpfennig et al. 2014; Shen et al. 2011). Earlier regional results indicated that a significant upward trend of mean annual temperature (MAT) coupled with CO_2 fertilization stimulated vegetation growth. Results from multiple studies have shown that the net primary productivity (NPP) of Chinese grassland increased by approximately 15−20% from 1980 to 2000, which is regarded as strong evidence for characterizing grasslands as a carbon sink (Fang et al. 2003; Ni 2000; Piao et al. 2003). During the past several decades, Chinese grasslands acted as a carbon sink overall, and this trend is predicted to continue for the next 100 years (Fang et al. 2007; Ji et al. 2008; Piao et al. 2007). However, more recent studies noticed that an increase in soil respiration and water consumption due to climate change could counteract the CO_2 fertilization effect and even reduce the current regional carbon sequestration in Chinese grasslands. Thus the carbon sequestration ability is likely to remain unchanged or even shrink in the future, especially in those arid and semiarid areas (Lu et al. 2009; Piao et al. 2012b; Sui and Zhou 2013).

Previous studies that investigated the responses of the regional terrestrial ecosystem to climate change were mostly based on categorization of the ecosystems by vegetation types, administrative division or geographic zoning (Fang et al. 2007; Liu et al. 2013; Ni 2002; Yang et al. 2008b). In those studies, however, the terrestrial water availability has not been explicitly identified, which could lead to confusion about carbon and water interactions and their impact on regional terrestrial ecosystems. For example, in the widely studied "arid/semiarid" area of Inner Mongolia, the water budget and the grassland types are diverse, ranging from the humid meadow steppe in the northeast to an extremely arid desert steppe in the southwest. Water availability varies greatly throughout the region, so the response of these diverse ecosystems to climate change should vary as well.

In this study, we modified and validated a terrestrial biogeochemical model, the boreal ecosystem productivity simulator (BEPS) (Chen et al. 1999), to simulate vegetation primary production (gross primary productivity [GPP], NPP), soil respiration (R_h), and net carbon sequestration ability (net ecosystem productivity [NEP]) in Chinese grasslands from 1982 to 2008. The model was modified to include the terrestrial carbon, hydrological, and nitrogen cycles and proved to work well in grassland ecosystems (Ju and Chen 2005; Ju et al. 2010; Matsushita and Tamura 2002; Zhang et al., 2013a, 2013b). In this study, we further modified some of the major model input parameters and algorithms to adjust the model to better simulate the regional grassland ecosystem (e.g., the maximum carboxylation rate [$V_{c,max}$], autotrophic respiration, production allocation). We divided Chinese grasslands into four subregions according to the aridity index (AI), and we studied the terrestrial response to climate change in response to different water budget levels. The goals of this study are to (1) investigate the spatiotemporal variation of the carbon sequestration ability in Chinese grasslands from 1982 to 2008 using a modified terrestrial ecosystem model and 2) quantify the response of Chinese grasslands to current climate variations (i.e., temperature and precipitation variations) at different terrestrial water budget levels (Fig. 1).

Methods

Model Description

In this study, we modified and applied a daily-step biogeochemical model, the BEPS. The model was initially developed to calculate vegetation GPP and NPP using the Farquhar leaf biochemical model and the canopy double-leaf scheme (Chen et al. 1999). A terrestrial hydrological model was incorporated to account for the soil water content (SWC) and evapotranspiration (Chen et al. 2007; Liu et al. 2003). In addition, a CENTURY-derived soil carbon and nitrogen model was introduced by Ju et al. (2006).

We modified the version of BEPS that includes all three modules mentioned earlier. In this paper, we only describe the major methods to calculate indexes of terrestrial carbon flux (i.e., NPP, heterotrophic respiration (R_h), and NEP), SWC simulation, and our modifications. A detailed introduction of the model can be found in the Supplementary Material.

The NEP is the difference between NPP and R_h:

$$NEP = NPP - R_h$$

where *NPP* is the difference between GPP and autotrophic respiration rate (R_a):

$$NPP = GPP - R_a$$

For the GPP simulation, the leaf maximum carboxylation efficiency ($V_{c,max}$) is an important input parameter that controls photosynthetic assimilation (Warren et al. 2003). Instead of using a predefined value, we used a multienvironmental limits scheme to calculate the $V_{c,max}$ with the Farquhar model according to Zhang and Zhou (2012):

$$V_{c,max} = V_{m,0} \times f(Temp) \times f(SW) \times f(CO_2) \times f(SN)$$

where $V_{m,0}$ is the maximum carboxylation rate under optimal environmental conditions and $f(Temp)$, $f(SW)$, $f(CO_2)$, and f(SN) are functions of the atmospheric temperature (Temp [°C]), surface SWC (SW [%]), atmospheric CO_2 concentration (CO_2 [Pa]), and soil nitrogen content (SN [mg/g]) that affects the $V_{c,max}$ value. R_a is simulated as the sum of growth respiration (R_g) and maintenance respiration (R_m). R_g is calculated as a fixed percentage from GPP. For R_m simulation, in the prototype model, we replaced the original Bonan (1995) algorithm with a plant component-specific scheme:

$$R_{m,k} = T_k \times r_{m,k} \times Q_{10,r}^{\frac{(T-T_{ref})}{10}}$$

T_k is the biomass of plant component k, and $r_{m,k}$ is the coefficient of the maintenance respiration. T and T_{ref} are air temperature and reference temperature for maintenance respiration, respectively. $Q_{10,r}$ is a temperature sensitivity factor for respiration calculated as a function of temperature (Arora 2003):

$$Q_{10,r} = 3.22 - 0.046T$$

After NPP has been simulated, a production allocation model is added according to Friedlingstein et al. (1999).

R_h is calculated by multiplying the carbon release rate (p_k) from the total carbon amount of a soil carbon pool (C_k).

$$R_h = \sum_{k=1}^{8} p_k C_k$$

For the R_h simulation, the major modifications of the soil module from the previous version were as follows: 1) The woody litter pool was excluded for grassland simulation and 2) the effect from soil moisture on decomposition (F_w) was calculated using the water-fill pore space (WFPS) according to the inTEC model ver. 3.0 (Ju and Chen 2005):

$$F_w = 5.44WFPS - 5.03WFPS^2 - 0.472$$

where *WFPS* is calculated as the ratio of SWC and saturated SWC.

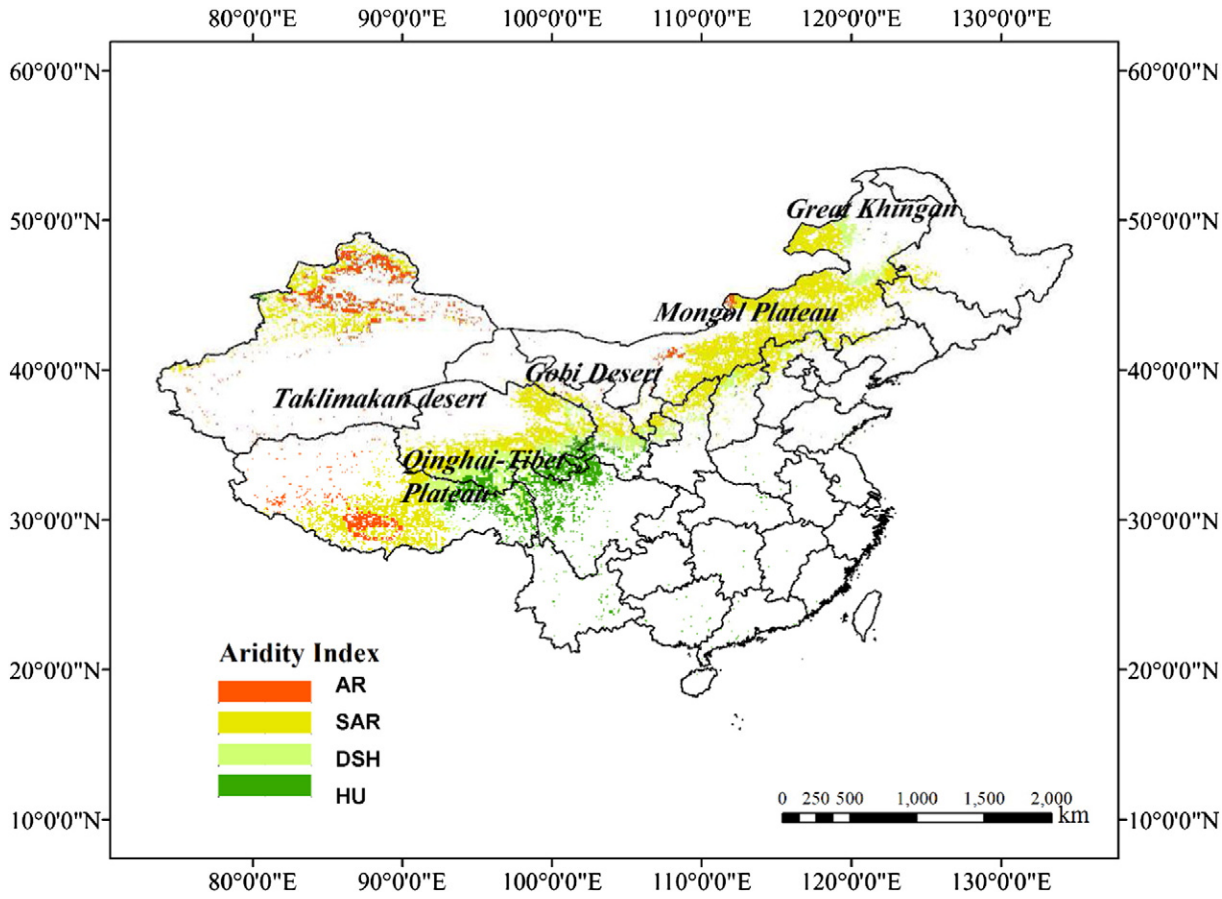

Fig. 1. Chinese grassland under different aridity levels.

The SWC is calculated by total water inputs (rainfall and snowfall) minus the total outputs (e.g., evapotranspiration, canopy interception, interlayer interaction, runoff). To accomplish this, the soil is separated into three layers and the canopy is divided into sunlit and sunshaded parts, the same as for the photosynthesis calculation. The SWC is related to the carbon cycle by defining the water stress effect on photosynthesis and soil respiration.

The revised grassland specific input parameters are shown in Table 1.

Data Preparation

Aridity Index (AI) Classification Map

We used the AI map from the Consultative Group for International Agriculture Research (CGIAR) from 2009 (aridity index dataset: http://www.cgiar-csi.org/data/global-aridity-and-pet-database). In this product, the AI was defined as the ratio of mean annual precipitation (MAP) to the Mean Annual Potential Evapotranspiration (MAPE):

$$AI = MAP/MAPE$$

MAP is obtained from the WorldClim Global Climate Data (Hijmans et al. 2005). The temporal scale is from 1950 to 2000. MAPE was modeled using the Hargreaves and Allen (2003) algorithm using the mean temperature and extraterrestrial radiation (RA), which was calculated by the method of Allen et al. (1998) method. The spatial resolution of the product is 0.008333 degrees. It was resampled into 8-km resolution.

According to the original dataset, terrestrial ecosystems are classified into five levels: hyper-arid (AI < 0.03, HAR), arid (0.03 < AI < 0.20, AR), semiarid (0.20 < AI < 0.50, SAR), dry and subhumid (0.50 < AI < 0.65, DSH), and humid (AI > 0.65, HU). However, few hyper-arid

Table 1
Grassland specific input parameters for the improved model.

Parameter Abbreviation	Original Value	Value	Description	Source
$V_{max,opt}$	/	100 (mmol m^{-2} s^{-1})	Optimal maximum rubisco-limited potential photosynthetic capacity	(Li et al., 2011)
SLA	0.015 (m^2 g^{-1})	0.025 (m^2 g^{-1})	Specific leaf area	(Schapendonk et al., 1998)
LR co.	0.008	0.002	Leaf respiration Coefficient	(Matsushita and Tamura, 2002)
SR co.	0.001	0.00005	Stem respiration Coefficient	(Matsushita and Tamura, 2002)
RR co.	0.003	0.0002	Root respiration Coefficient	(Matsushita and Tamura, 2002)

Chinese grasslands exist, so we combined that category with AR (see Fig. 1).

Model Input Data

Land Cover Map

The MODIS land cover product (USGS-EROS, MODIS product, MOD12Q1-2001, Available at: https://lpdaac.usgs.gov) was used due to its good quality and wide usage. We used the version with IGBP global vegetation classification and 1-km resolution. Chinese grassland map was extracted and resampled to 8-km resolution to fit for the model input.

LAI

We used a daily-step 8-km LAI product (CAS, Global LAI database, Available at: http://www.globalmapping.org/globalLAI/) to drive the model. The consistent 8-km daily LAI product was derived from both Moderate Resolution Imaging Spectroradiometer (MODIS) and Advanced Very High Resolution Radiometer (AVHRR) products. The MODIS LAI series was generated using GLOBCARBON LAI algorithm for the period since 2000 (2000–2008 in this study). Thereafter, the relationships between AVHRR SR and MODIS LAI were established pixel by pixel during the overlapped period (2000–2006). On the basis of these relationships, homogeneous LAI series were retrieved from historical AVHRR observations for the period before 2000 (1982–1999 in this study). More details can be found in Liu et al. (2012).

Daily Meteorological Data

The daily air temperature, precipitation, radiation, and specific humidity are required to drive the model. We used the Global Meteorological Forcing Dataset for Land Surface Modeling (Princeton University, Global Meteorological Forcing Dataset for Land Surface Modeling, Available at: http://rda.ucar.edu/datasets/ds314.0/). This database is based on global observation datasets and NCEP/NCAR reanalysis, and to enhance its accuracy, it was recently updated with the results from the World Meteorological Organization (WMO) Solid Precipitation Measurement Inter-comparison and Global Precipitation Climatology Project (GPCP) daily product. Thereafter, the data were evaluated by using the second Global Soil Wetness Project (GSWP-2) dataset and 753 basic meteorological stations across China. The spatial resolution is 8 km.

Atmospheric CO_2 Data

Monthly atmospheric CO_2 data were collected from Mauna Loa Observatory (MLO), Hawaii (20°N, 156°W) (MLO, Air CO_2 database, Available at: http://cdiac.esd.ornl.gov/ftp/trends/co2/maunaloa.co2).

Soil Texture Data

Soil texture data were collected from the Global Soil Dataset for use in Earth System Models (GSDE, Available at: http://globalchange.bnu.edu.cn/research/soilw). The data are displayed in the volumetric percentages of silt, clay, and sand, from which hydrological parameters including the wilting point, field capacity, soil porosity, and maximum water-holding capacity can be estimated. The spatial resolution is 1 km.

All the input datasets were extracted and resampled to 8 km to fit for the model simulation.

Model Simulation and Data Analysis

The model uses a semianalytical scheme to calculate the steady state of soil carbon storage (Ju et al. 2006; Xia et al. 2012). First it calculates the regional quasi-steady-state pool sizes by setting the terrestrial flux equal to zero to ensure that the pools' sizes are close to the assumed steady state without running the model for hundreds or thousands of years. Next, the pools are further spun up by using mean historical forcing data to meet the steady-state criterion. The run time depends on the carbon residence time in the various pools. In this study, we used the daily climatic data during 1948–1953 and a corresponding CO_2 concentration of 311 ppm to execute the initialization. Finally, we ran the model with transient climatic forcing and a rising CO_2 concentration to obtain the carbon storage level at the beginning of 1982. During this period, LAI was estimated using the specific leaf area (SLA, the ratio of leaf area to leaf biomass) and simulated leaf biomass. A parameter of maximum LAI was used to constrain the LAI upper limit. After that, the model was run again with the historical LAI and meteorological inputs from 1982 to 2008 with a daily step.

We defined a linear regression model $y = a + bx$ to analyze the spatiotemporal trend of GPP, NPP, and NEP, where x represents the study year.

A one-way analysis of variance (ANOVA) was used to test the significance of correlationships between ecosystem indexes (i.e., NPP, NEP, and R_h) and climatic factors (i.e., MAP and MAT) using SPSS 20.0 (IBM SPSS Inc., Chicago, IL, USA). Differences at $p < 0.05$ and $p < 0.01$ were considered as significant and very significant, respectively.

Model Validation

Simulation results for both the original and modified models were compared with EC measurements and field work results (Table 2).

The two Eddy Covariance (EC) sites are located at Xilinhot (IM) and Tongyu (TY) (Chen et al. 2009; Yang et al. 2008a). Daily-step data for GPP and net ecosystem emission (NEE, equal to −NEP) with complete meteorological information were used to evaluate the corresponding model results.

Field measurements of biomass were collected from major grasslands in China, including grasslands in Xinjiang, Inner Mongolia and on the Qinhai-Tibet Plateau. Each of these sites represents a typical vegetation pattern in a local area. The biomass data were sampled from four replicates within each test site. The total biomass was defined as the sum of the herbaceous, litter, and root biomass. The peak-season living aboveground biomass and litter was measured by the destructive sampling of 1.0 m^2. The recent litters were selected. Thereafter, the samples were dried at 65°C to constant weight and then weighted. Roots were collected by excavating 1.0 m^2 squares to a depth of 0.5 m. Root matters were hand sorted from soil, washed, dried at 65°C, and weighted. The dry matter values were converted to carbon assuming a proportional factor of 0.475 (Garbulsky and Paruelo 2004).

Information about the sites can be found in Table 2.

Results

Model Validation and Comparison

The modified model had better performance than the original model for both comparisons with the EC sites and field studies (Figs. 2 and 3). For the EC sites, the average R^2 values of GPP (GPP_{MOD}) against GPP from EC measurements (GPP_{EC}) were increased by 0.15 (0.77 and 0.83 for the revised model compared with 0.64 and 0.66 for the original model in IM and TY, respectively). The average R^2 increase in the net ecosystem emission (NEE, equal to −NEP) was 0.11 (0.84 and 0.78 for the revised model compared with 0.73 and 0.68 for the original model in IM and TY, respectively). The average RMSE values of GPP decreased by 0.66 $gC.m^{-2}$ (1.25 $gC.m^{-2}$ and 1.4 $gC.m^{-2}$ for the revised model compared with 1.99 $gC.m^{-2}$ and 1.96 $gC.m^{-2}$ for the original model in IM and TY, respectively), and the value decreased by 0.21 $gC.m^{-2}$ for NEE (0.96 $gC.m^{-2}$ and 0.92 $gC.m^{-2}$ for the revised model compared to 1.21 $gC.m^{-2}$ and 1.1 $gC.m^{-2}$ for the original model in IM and TY, respectively). The modified model also showed a better correlation with the field NPP ($R^2 = 0.79$ for the modified model against 0.76 for the original model, $P < 0.001$, see Fig. 3).

On the basis of these statistics comparisons, we believe that our modifications could improve the model performance for Chinese grasslands. The model results are credible and suitable for this regional study.

Table 2
List of site information for model validation.

Site	Data type	Long.	Lati.	Climate*	Time extent	Number of samples
IM	FLUX	116°40'E	43°33'N	BSk	2004	/
TY	FLUX	122°52'E	44°25'N	Dwa	2008	/
Northern Tibet	Field	100°51'-101°17'E	36°57'-37°36'N	ET	2004-2007	49
Xinjiang	Field	88°37'E-88°40'E	44°29'N-44°31'N	Bwk	2012	52
Inner Mongolia	Field	111°6'3"E-118°20'24"E	42°19'12"N −46°9'36"N	BSk, Dwb	2004-2008	54

* Climate type of grassland is based on Koeppen-Geiger classification (http://koeppen-geiger.vu-wien.ac.at/). BSk: main climate — arid, precipitation — steppe and temperature — cold arid; Dwa: main climate — snow, precipitation — desert and temperature — hot arid; ET: main climate — polar and temperature — polar tundra; Bwk: main climate — arid, precipitation — desert and temperature — cold arid; Dwb: main climate — snow, precipitation — desert, temperature — warm summer.

Spatiotemporal Pattern of GPP, NPP, and NEP at Different AIs

Fig. 4 shows the spatial distribution of the mean annual value, slope (b), and correlation coefficient (r) of GPP, NPP, and NEP in China from 1982 to 2008. GPP and NPP have similar spatial distributions and variation trends for Chinese grasslands, indicating a relatively stable autotrophic respiration level. Grassland production has a clear zonal distribution from near-forest to near-desert. High-productivity grasslands are mainly located in HU, DSH, and those SAR areas connected to forests, such as the meadow steppe joined to Great Khingan and Siberia Forest in the eastern and southeastern part of the Mongol Steppe, and the alpine meadow near the southern and eastern part of the Qinghai-Tibet Plateau. The values for those areas are generally above 200 and 150 gC.m^{-2} per year for GPP and NPP, respectively. These parts are also among the fastest-growing areas with a significant positive trend (see Fig. 4b and c). Grasslands with lower productivity are those areas near the Gobi and Taklimakan deserts, for which GPP and NPP are typically < 20 and 10 gC.m^{-2} per year, respectively. A large part of these areas also experienced a significant production increase; however, the absolute value was strongly limited by the environmental condition and the intrinsic vegetation growth potential. The main reductions were concentrated around the northwestern part of the Tibet-Qinghai Plateau and the northeastern corner of Inner Mongolia extending to the central part, but the decreasing trend was mostly insignificant.

NEP calculated by the model has a similar spatial distribution to NPP. Chinese grasslands mainly acted as a carbon sink during the 27 years under consideration (see Fig. 4a). Strong sink areas are those with high productivity, and weak sink or source areas are those with low productivity. The regional temporal trend showed a divergence with production (see Fig. 4c). A decreasing trend was found in the northern part of Xinjiang Province, the northern and eastern part of Inner Mongolia, and the southeastern part of the Qinghai-Tibet Plateau. However, only small parts of these areas showed significant changes. A significant increasing tendency was found in the SAR areas near Taklimakan desert and in southern Inner Mongolia.

Temporal Variations of Meteorological Factors and Terrestrial Carbon Flux Indexes

During the research period, the entire region's MAT increased by approximately 1.3°C according to the fitted linear regression equation, showing significant trends in all four subregions (Fig. 5a). However, no significant MAP trend was found except a slight increase in the AR region (Fig. 5b). Under such environmental conditions, Chinese grasslands' productivity increased in all AI zones. The overall

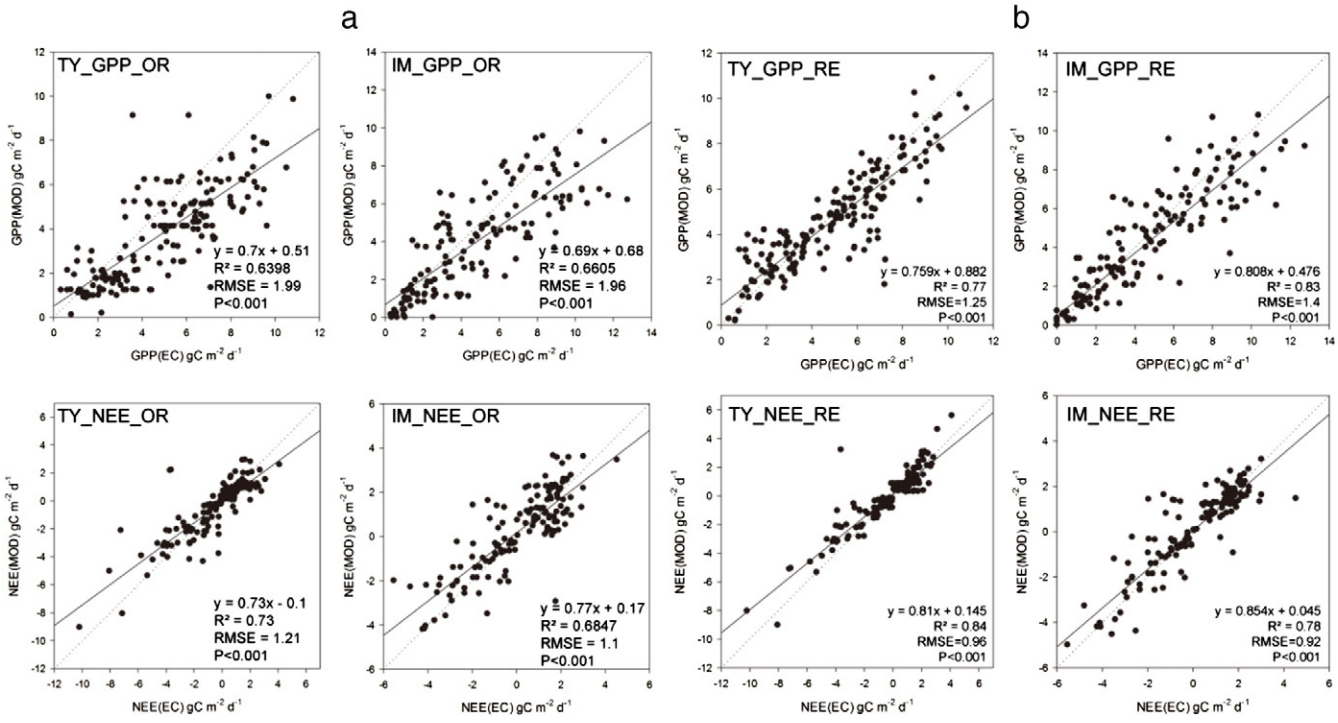

Fig. 2. Comparisons of modeled GPP (GPP_{MOD}, gC.m^{-2}.d^{-1}) and NEE (NEE_{MOD}, gC.m^{-2}.d^{-1}) to daily EC sites' measurements in Tongyu (TY) and Inner Mongolia (IM): (a) the results with the original model (OR); (b) the results with revised model (RE). The unit of RMSE is gC.m^{-2}.

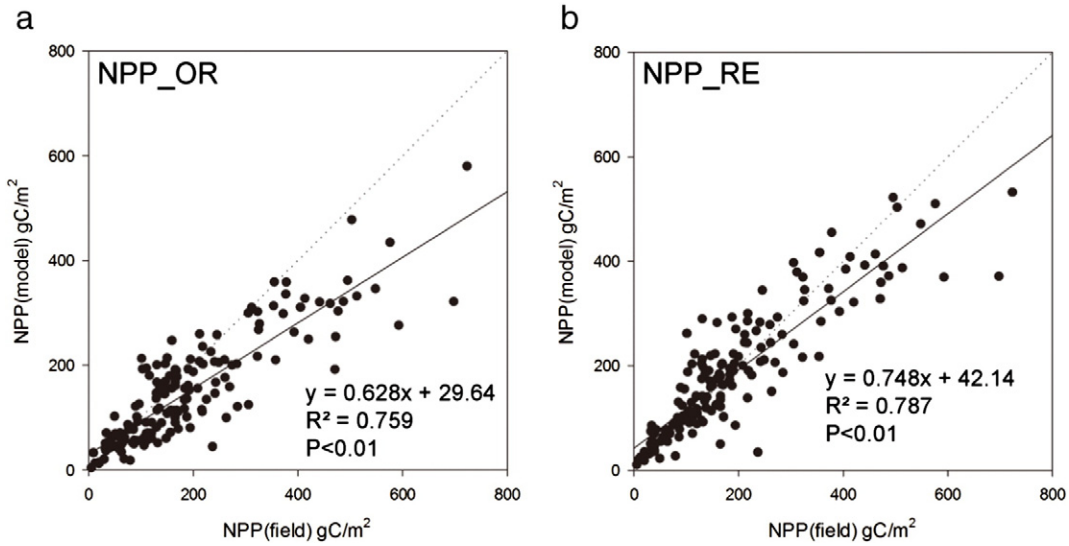

Fig. 3. Comparison between modeled NPP (NPP_{MOD}, $gC.m^{-2}$) and observed NPP (NPP_{Field}, $gC.m^{-2}$) from independent field measurements collected from Inner Mongolia, Qinghai-Tibet Plateau and Xingjiang: (a) the result with the original model (OR); (b) the result with revised model (RE).

increments were about 50.1 $gC.m^{-2}$ and 36.1 $gC.m^{-2}$ for GPP and NPP, respectively (Fig. 5c and d). However, during the period, NEP showed a continuous fluctuation without any significant trend (Fig. 5e).

Impact of Changes in Meteorological Factors on NPP, R_h, and NEP

The responses of NPP and R_h to climate change in the different AI zones are shown in Table 3. Significant relationships exist between NPP and MAT in HU, DSH, and SAR zones, with relatively good explanation ability. Slope increases from SAR to HU from 12.33 to 29.18 were evident. R_h also showed significantly positive correlation with MAT in all AI zones and slope increases from AR to HU from 6.50 to 26.91.

The linear correlations between NPP and MAP become progressively weaker from the arid end to the humid end. Significant correlations were found for AR and SAR but not for DSH and HU. In contrast, we did not find a significant correlation between R_h and MAP across the entire range of AI levels.

Moreover, no direct correlation was found between NEP and MAT or MAP.

Discussions

Our modified model performed better for grasslands than the original BEPS model at both EC sites and for field measurement comparisons. From a regional perspective, our NPP result is generally consistent with the results of major models but much less than the result from the CASA model (Potter et al. 1993) (Table 4). However, it seems that the original CASA model overestimated NPP because the value declined significantly after an improvement by Xing et al. (2010) and was close to our result as well. For NEP, we found that our result was similar to the result from the GLPM and slightly higher than the result from the TEM. The main reasons for these differences could be the longer study period in the Sui study (1951–2007), which covered 3 decades during which NEP was lower than in recent times. Furthermore, different model inputs could also influence the results. Our result is much higher than that derived from the grassland resource inventory. We think that the use of different methods to calculate vegetation production is one of the main reasons for the discrepancy in the results. In the work of Fang et al. (2007), the aboveground biomass was directly estimated via a statistical model from the annual maximum NDVI and the grassland biomass C density, and the C content was derived from the biomass using a factor of 0.45. Belowground biomass is estimated by a predefined root-to-shoot ratio for each grassland type. However, for BEPS and similar terrestrial biogeochemical models, the total carbon input is estimated by the Farquhar biochemical model or a light-use efficiency scheme and ecosystem respiration is estimated using a multipool scheme. This mechanical difference in estimation methodology has produced large discrepancies in regional studies. According to the study by Piao et al. (2012a), an estimation using the ensemble terrestrial ecosystem model (without considering biofuel consumption) is higher than the result from the inventory method for East Asia (-0.413 ± 0.141 Pg $C.yr^{-1}$ vs. -0.293 ± 0.033 Pg $C.yr^{-1}$). Moreover, the different land cover classifications could also account for the discrepancies. In Fang's study, more barren regions were classified as grasslands, especially arid/semiarid areas located in Central and Northwestern Tibet (close to the Taklimakan Desert). These areas are characterized as desert steppe and have a very low carbon density and sequestration potential.

In this study, the AI classification distinguishes Chinese grasslands with different aridity levels and reveals the different situations, trends, and responses to climate change. Induced by various biogeographic features of grasslands in different AI zones, the response pattern of the grasslands to hydrothermal conditions varies. Different responses from grassland to MAP could be explained by a change in the major limitation for vegetation growth. For relatively humid areas, precipitation is always sufficient for regular vegetation growth and transpiration, so too much water input can induce ineffective water use and a higher biogeochemical requirement, such as a nutrient limitation (Austin and Vitousek 1998). For arid/semiarid areas, vegetation production is seriously limited by water scarcity and induces vegetational limitations such as low LAI and high root-to-shoot ratio (Bai et al. 2010; Fan et al. 2009). Thus vegetation production is much more sensitive to water availability in such areas. Our results for arid/semiarid areas are in accordance with those of Yang et al. (2010) and Ni (2004a), who also noted a significant positive correlation between NPP and MAP. In contrast, we do not find a direct correlation between MAP and R_h. One possible explanation is that MAP hardly represents the true soil moisture conditions because moisture is consumed by other means such as evapotranspiration or runoff and less is conserved in the soil, especially in arid/semiarid areas. In addition, the intra-annual precipitation distribution could have a profound impact on this response. If more extreme rainfall events occur, the actual period for which the soil water content is suitable could be reduced in humid ecosystems, while it could be prolonged in arid ecosystems. This mechanism has been theoretically explained and demonstrated by multiple studies and might contribute to the ambiguous relationship between MAP and R_h (Jentsch and Beierkuhnlein 2008; Knapp et al. 2008; Luo et al. 2008). For MAT,

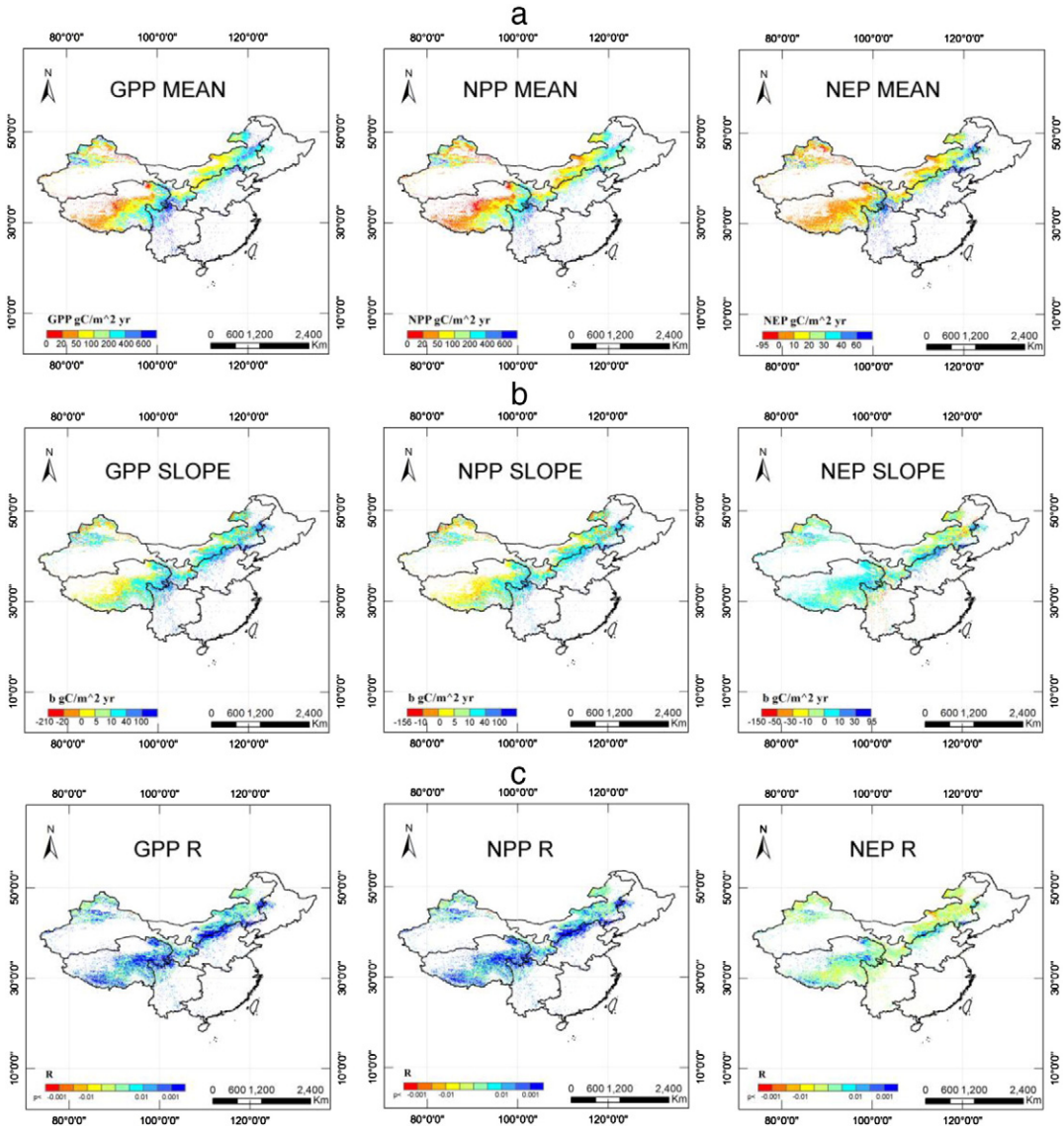

Fig. 4. Spatial distribution of (a) mean annual value (MEAN), (b) annual change rate (SLOPE) and (c) correlation coefficient (R) of GPP, NPP and NEP during the period from 1982 to 2008. Positive (negative) values of SLOPE and R represent increase (decrease) of the corresponding index; p values represent significant levels.

significant positive production correlations were found in most areas, except for the AR zone. This suggests that a difference still exists between the present temperature conditions and optimal temperature conditions for grass growth. According to the results from Piao et al. (2006a) and Parmesan (2007), an overall increase in temperature could promote earlier greening and extend the growth season in temperate grasslands, especially in these areas that have a high growth potential (Knapp and Smith 2001). Additionally, higher temperatures could also promote soil N mineralization and therefore benefit the nutrition supply for vegetation (Melillo et al. 2002).

Chinese grasslands mainly consist of SAR (>50%) with the largest amount of carbon sequestration of approximately 16.4 TgC per year and the HU zone with approximately 9.5 TgC per year. These two zones comprise the major contributors to the carbon sink in Chinese grasslands. Under the current trend of climate warming, a concurrent increase in vegetation production and soil respiration leads to a fluctuation in carbon sequestration. We did not find a direct relationship between NEP and MAT, but significant a positive correlation between NPP/R_h and MAT was found, and the R_h was found to increase more quickly than NPP in the AR and SAR zones (70% of the entire area) but more slowly in the DSH and HU zones (≈30% of the entire area) as MAT increased. Then, we calculate the net increase of MAT-driven NPP and R_h over the entire region by multiplying them by the areas of each AI (we assumed that no NPP variation occurred in AR with a MAT increase). The results showed that Chinese grasslands could lose 1.29 TgC per year with each 1°C rise in MAT, which means that regional warming will lead to larger differences in carbon sequestration between arid and humid grasslands and an overall reduction of the grassland carbon sequestration ability. The result is in accordance with previous studies by Piao et al. (2012b) and Lu et al. (2009), who also remarked that without the influence of other unforeseen factors, grassland carbon fixation ability will probably weaken due to climatic warming in the future, especially in arid/semiarid areas. A possible increase in precipitation during the growth season may slightly mitigate this trend by stimulating productivity in the AR and SAR zones. But the extra water input may also indirectly stimulate the microbial respiration by creating a more suitable soil environment (Janssens and Pilegaard 2003; Peng et al. 2009; Zheng et al. 2009).

The current atmospheric CO_2 concentration is not at the saturation point for plant photosynthesis, so an increase could still cause increased biomass accumulation, which has been demonstrated in some regional studies (Piao et al. 2006b; Sitch et al. 2013). At the same time, the

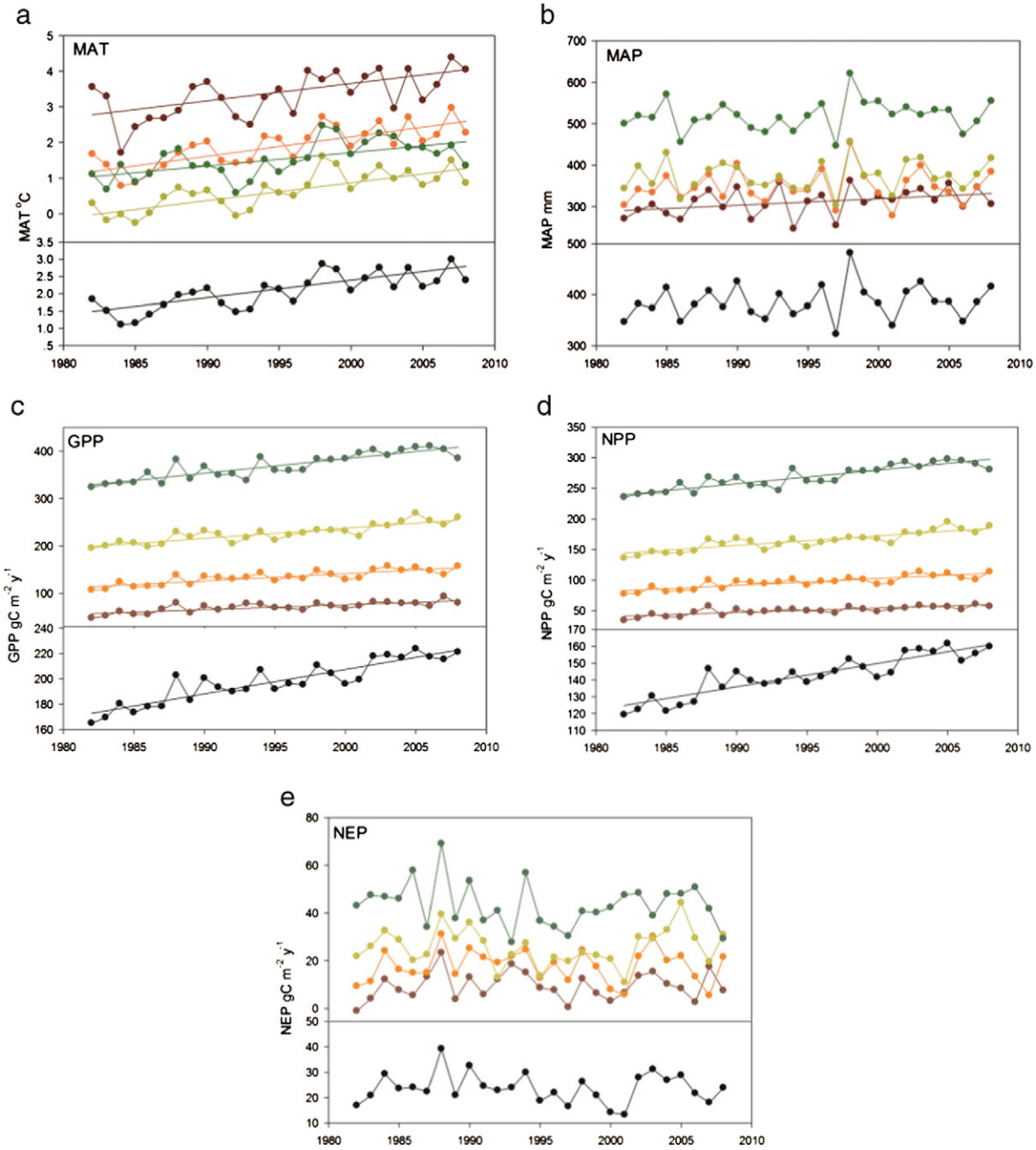

Fig. 5. Temporal trends of (a) MAT(°C), (b) MAP (mm), (c) GPP ($gC.m^{-2}.yr^{-1}$), (d) NPP ($gC.m^{-2}.yr^{-1}$) and (e) NEP ($gC.m^{-2}.yr^{-1}$) in different AI zones during the period from 1982 to 2008. Green lines represent HU zone, yellow lines represent DSH zone, orange lines represent SAR zone, maroon lines represent AR zone and black lines represent regional means. The solid straight lines represent that the significant linear trend ($p < 0.05$) exists during the period.

Table 3
Linear correlationships between annual NPP/R_h and MAT/MAP.

	MAP			MAT		
NPP	Equation	R^2	p	Equation	R^2	p
AR	$y = 0.1498x + 4.0693$	0.4014	<0.001			N
SAR	$y = 0.1067x + 59.78$	0.1558	<0.05	$y = 12.328x + 73.522$	0.4251	<0.001
DSH			N	$y = 19.695x + 151.71$	0.5139	<0.001
HU			N	$y = 29.182x + 223.81$	0.5107	<0.001
R_h	Equation	R^2	p	Equation	R^2	p
AR			N	$y = 6.4972x + 19.678$	0.5426	<0.001
SAR			N	$y = 13.473x + 53.486$	0.6622	<0.001
DSH			N	$y = 18.742x + 126.56$	0.6309	<0.001
HU			N	$y = 26.907x + 183.79$	0.455	<0.001

"N" represents no significant relationship exists, i.e. $p > 0.05$.

Table 4
Result comparison between recent studies and this paper of Chinese grassland's NPP ($gC.m^{-2}.yr^{-1}$) and NEP ($gC.m^{-2}.yr^{-1}$).

Study area	Study period	Method	Results ($gC.m^{-2}.yr^{-1}$)	Corresponding results in this paper* ($gC.m^{-2}.yr^{-1}$)	reference
Northern China	2000-2005	Improved CASA model	NPP:153.26	143.4	(Xing et al., 2010)
China	2000	CASA	NPP:245	141.58	(Gao and Liu, 2008)
		CEVSA	NPP:208		
		GLOPEM	NPP:145		
		GEOLUE	NPP:178		
		GEOPRO	NPP:168		
China	2007	BEPS	NPP: 122.6	155.72	(Feng et al., 2007)
Xilin River basin, Inner Mongolia	2002	GLPM	NEP:1.91	2.23	(Zhang et al., 2009)
Inner Mongolia	1951-2007	TEM	NEP:11.25	15.97 (from 1982 to 2007)	(Sui et al., 2013)
China	1981-2000	Chinese Grassland resource inventory	NEP:2.12	5.65 (from 1982 to 2000)	(Fang et al., 2007)

* the results are extracted from the simulated map in this study with the same spatiotemporal scale to the corresponding recent studies. The results are mean annual values of the corresponding study period.

studies in both recent decades and future predictions agree that the greatest part of the carbon sink attributed to a rise in CO_2 is distributed in Southeast China (Sui et al. 2013; Wang et al. 2014). Hence this response pattern may contribute to larger differences in carbon sequestration between arid and humid areas. Moreover, it should be noted that CO_2 fertilization may only play a minor role in the NEP variation of Chinese grasslands. For example, Mu et al. (2008) indicated that although CO_2 fertilization could have a strong impact on the Chinese carbon sink, its impact on grasslands is the weakest and only accounts for 0.3% of the total NPP. The results from the TEM showed that CO_2 fertilization could only counteract 1.4% of a NEP decrease while the climatic factor caused a NEP variation of 15.3% (Sui et al. 2013).

N deposition could enhance photosynthesis input by increasing the leaf nitrogen levels and decelerate soil carbon decomposition by raising the ratio of C and N in soil pools. According to a summary by Piao et al. (2012a), N deposition could lead to an increase in carbon sequestration in China ranging from −0.125 Pg C to < −0.089 Pg C. Currently, most studies on Chinese grasslands are focused on semiarid temperate steppes (e.g., Inner Mongolia), while little work has been done on grassland areas on a national scale. The limitations come from a paucity of field research and the existence of large uncertainties in nitrogen-coupled model simulations (Liu et al. 2011).

By incorporating LAI to drive the model, we implicitly include the impacts from some major disturbances in grasslands, such as grazing, mowing, and fire. On the basis of this calculation, vegetation responses to disturbances are actually added into the production prediction and the bias range could largely depend on how much productivity is consumed or lost to the disturbances. In the past 30 years, the number of livestock in China has exploded. According to our previous research in Inner Mongolia, the total number of livestock in 2010 more than doubled from that in 1986 (≈100 million head vs. 40 million head, respectively), which largely aggravated grazing and mowing pressure on grasslands and led to continuous degradation (Mu et al. 2013). This situation is currently common in the SAR and AR zones in China, such as in the temperate steppe in the Mongol Plateau and the alpine meadow grasslands in the northwestern part of the Qinghai-Tibet Plateau (Li et al. 2005; Li et al. 2006). According to the surveys of Liu et al. (2004), approximately 90% of Chinese natural grasslands is degraded to various extents. As one thing leads to another, this trend will finally result in an undesirable transformation of the land cover from grasslands to sand land or desert (Pei et al. 2008). In addition, other disturbances such as mining and fires on grasslands are predicted to increase (Liu and Diamond 2005; Stephens et al. 2014; Wang et al. 2013). Thus a direct loss in productivity major perturbations increased from the 1980s to 2000s, and these trends will probably continue in the future due to the increasing demands of animal production (McMichael et al. 2007). Because the aggravation of regional degradation has been noted in major Chinese pasture areas (especially during the period 1980–2000) (Zhang et al., 2013a), we think that regional disturbances negatively affect grassland ecosystems. Therefore the pure NPP responses to climate change are actually greater than our current calculations indicate. This bias could also be present in former regional simulations and predictions based on diagnostic models because the model inputs for canopy data are similar (e.g., LAI, NDVI, vegetation coverage) for representing photosynthetic capacity and vegetation growth. Therefore we think that stronger production responses to climate change should be noted in future studies, and a comprehensive description of terrestrial biogeochemical cycle responses to disturbances is urgently needed for large-scale ecosystem carbon budget modeling and calculations.

Land use and cover change (LUCC) is another unpredictable factor. The current LUCC is closely related to human activity and government policies. On the one hand, inappropriate human use and activities, in addition to the increasing frequency of extreme climatic events (e.g., drought, snowstorms), have contributed to grassland degradation in arid/semiarid areas, as discussed in the previous paragraph. On the other hand, the Chinese government has instituted several large regional programs to address these problems since the late 1990s. One of the most well-known projects is the Grain to Green Project (GTGP), which has induced a land conversion from deserts and croplands to grasslands or forests (Wang et al. 2007). Reports indicate that the grassland area increased by 77,993 km^2 from 2000 to 2009, with 29,432.71 Gg C. yr^{-1} in Inner Mongolia (Mu et al. 2013). A similar trend has been reported for Shanxi, Gansu, Qinghai, and Xinjiang provinces (Feng et al. 2005). Moreover, the current trend of urbanization has accelerated the expansion of urban areas to original natural ecosystems, and this process also moves a large amount of the rural population to the cities, thus contributing to the recovery of grasslands and shrublands in rural areas (Pärtel et al. 2007; Peng et al. 2009). According to a summary by Liu et al. (2010), climate warming and the pursuit of economic profits are the major drivers of grassland reduction, while large ecological projects, for example, the GTGP, drive grassland expansion in China. Therefore we think that a combination of these factors accounts for part of the large uncertainty regarding carbon sequestration in Chinese grasslands.

Above all, on the basis of our predictions, the carbon sink ability of Chinese grasslands will continue to fluctuate in the future, but a danger exists that this sink might be minimized because of multiply factors.

Implications

According to the results from our model, under current climate change trends, grassland production increased in all AI zones from 1982 to 2008. However, because soil respiration was simultaneously increased, the grassland carbon sequestration ability fluctuated and did not show a significant trend. Meanwhile, grassland production was only sensitive to MAP in arid/semiarid areas, while a higher MAT led to production increases in a wider range of grasslands because of the large difference between present temperature conditions and the optimum temperature conditions for grasslands. The warming trend led to an R_h increase as well. However, no direct correlation was

found between NEP and MAP or MAT. On the basis of these results, we predict that a danger exists: Chinese grasslands may exhibit a lower carbon sequestration ability in the future in response to multiple factors, including those arising from terrestrial biogeochemical cycles, disturbances, and LUCC. The difference between the carbon sequestration ability between arid and humid zones will probably increase. In addition, we also suggest that to accurately quantify regional carbon sequestration ability and its responses to climate change, a comprehensive disturbances model should be incorporated into current terrestrial ecosystem modeling.

This paper could contribute to an in-depth understanding of carbon sequestration and response mechanisms in Chinese grasslands under a background of global change and be a reference for policy makers to use in the development of further plans and projects to protect grasslands and preserve their functions in terrestrial carbon circulation.

Acknowledgments

We are sincerely grateful to the editor and anonymous reviewers. We also greatly acknowledge Dr. Ju Weimin from Nanjing University to offer the original model, data, and instructions; Dr. Shi Zheng from Oklahoma University to suggest revisions for the paper; and Dr. Fu Congbin and Dr. Meng Xiangxin from the Chinese Academy of Science to provide EC data in Tongyu. Without their kind help, this work would not have been finished.

References

Allen, R.G., Pereira, L.S., Raes, D., Smith, M., 1998. Crop evapotranspiration—Guidelines for computing crop water requirements-FAO Irrigation and drainage paper 56. 300. FAO, Rome, p. 6541.

Arora, V.K., 2003. Simulating energy and carbon fluxes over winter wheat using coupled land surface and terrestrial ecosystem models. Agric. For. Meteorol. 118, 21–47.

Austin, A.T., Vitousek, P., 1998. Nutrient dynamics on a precipitation gradient in Hawai'i. Oecologia 113, 519–529.

Bai, Y., Zhang, W., Jia, X., Wang, N., Zhou, L., Xu, S., Wang, G., 2010. Variation in root: shoot ratios induced the differences between above and belowground mass–density relationships along an aridity gradient. Acta Oecol. 36, 393–395.

Bonan, G.B., 1995. Land-atmosphere CO_2 exchange simulated by a land surface process model coupled to an atmospheric general circulation model. J. Geophys. Res. 100, 2817–2831.

Calzadilla, A., Rehdanz, K., Betts, R., Falloon, P., Wiltshire, A., Tol, R.S.J., 2013. Climate change impacts on global agriculture. Clim. Chang. 120, 357–374.

Cao, J.-J., Xiong, Y.-C., Sun, J., Xiong, W.-F., Du, G.-Z., 2011. Differential benefits of multi- and single-household grassland management patterns in the Qinghai-Tibetan Plateau of China. Hum. Ecol. 39, 217–227.

Chen, J., Liu, J., Cihlar, J., Goulden, M., 1999. Daily canopy photosynthesis model through temporal and spatial scaling for remote sensing applications. Ecol. Model. 124, 99–119.

Chen, B., Chen, J.M., Ju, W., 2007. Remote sensing-based ecosystem–atmosphere simulation scheme (EASS)—Model formulation and test with multiple-year data. Ecol. Model. 209, 277–300.

Chen, S., Chen, J., Lin, G., Zhang, W., Miao, H., Wei, L., Huang, J., Han, X., 2009. Energy balance and partition in Inner Mongolia steppe ecosystems with different land use types. Agric. For. Meteorol. 149, 1800–1809.

Duan, Q., Xin, X., Yang, G., Chen, B., Zhang, H., Yan, Y., Wang, X., Zhang, B., Li, G., 2011. Current situation and prospect of grassland management decision support systems in China. Computer and computing technologies in agriculture IV. Springer, New York, NY, USA, pp. 134–146.

Falkowski, P., Scholes, R., Boyle, E.A., Canadell, J., Canfield, D., Elser, J., Gruber, N., Hibbard, K., Högberg, P., Linder, S., 2000. The global carbon cycle: a test of our knowledge of earth as a system. Science 290, 291–296.

Fan, L.-Y., Gao, Y.-Z., Brück, H., Bernhofer, C., 2009. Investigating the relationship between NDVI and LAI in semi-arid grassland in Inner Mongolia using in-situ measurements. Theor. Appl. Climatol. 95, 151–156.

Fang, J., Piao, S., Field, C.B., Pan, Y., Guo, Q., Zhou, L., Peng, C., Tao, S., 2003. Increasing net primary production in China from 1982 to 1999. Front. Ecol. Environ. 1, 293–297.

Fang, J., Guo, Z., Piao, S., Chen, A., 2007. Terrestrial vegetation carbon sinks in China, 1981–2000. Sci. China Ser. D Earth Sci. 50, 1341–1350.

Feng, X., Liu, G., Chen, J., Chen, M., Liu, J., Ju, W., Sun, R., Zhou, W., 2007. Net primary productivity of China's terrestrial ecosystems from a process model driven by remote sensing. Journal of Environmental Management 85, 563–573.

Feng, Z., Yang, Y., Zhang, Y., Zhang, P., Li, Y., 2005. Grain-for-green policy and its impacts on grain supply in West China. Land Use Policy 22, 301–312.

Friedlingstein, P., Joel, G., Field, C., Fung, I., 1999. Toward an allocation scheme for global terrestrial carbon models. Glob. Chang. Biol. 5, 755–770.

Gao, Z., Liu, J., 2008. Simulation study of China's net primary production. Chinese Science Bulletin 53, 434–443.

Garbulsky, M.F., Paruelo, J.M., 2004. Remote sensing of protected areas to derive baseline vegetation functioning characteristics. J. Veg. Sci. 15, 711–720.

Gosling, S.N., Arnell, N.W., 2013. A global assessment of the impact of climate change on water scarcity. Clim. Chang. 1–15.

Hargreaves, G., Allen, R., 2003. History and evaluation of Hargreaves evapotranspiration equation. J. Irrig. Drain. Eng. 129, 53–63.

Hijmans, R.J., Cameron, S.E., Parra, J.L., Jones, P.G., Jarvis, A., 2005. Very high resolution interpolated climate surfaces for global land areas. Int. J. Climatol. 25, 1965–1978.

Janssens, I.A., Pilegaard, K., 2003. Large seasonal changes in Q_{10} of soil respiration in a beech forest. Glob. Chang. Biol. 9, 911–918.

Jentsch, A., Beierkuhnlein, C., 2008. Research frontiers in climate change: effects of extreme meteorological events on ecosystems. Compt. Rendus Geosci. 340, 621–628.

Ji, J., Huang, M., Li, K., 2008. Prediction of carbon exchanges between China terrestrial ecosystem and atmosphere in 21st century. Sci. China Ser. D Earth Sci. 51, 885–898.

Ju, W., Chen, J.M., 2005. Distribution of soil carbon stocks in Canada's forests and wetlands simulated based on drainage class, topography and remotely sensed vegetation parameters. Hydrol. Process. 19, 77–94.

Ju, W., Chen, J.M., Black, T.A., Barr, A.G., Liu, J., Chen, B., 2006. Modelling multi-year coupled carbon and water fluxes in a boreal aspen forest. Agric. For. Meteorol. 140, 136–151.

Ju, W., Chen, J.M., Black, T.A., Barr, A.G., McCaughey, H., 2010. Spatially simulating changes of soil water content and their effects on carbon sequestration in Canada's forests and wetlands. Tellus B 62, 140–159.

Knapp, A.K., Smith, M.D., 2001. Variation among biomes in temporal dynamics of aboveground primary production. Science 291, 481–484.

Knapp, A.K., Beier, C., Briske, D.D., Classen, A.T., Luo, Y., Reichstein, M., Smith, M.D., Smith, S.D., Bell, J.E., Fay, P.A., 2008. Consequences of more extreme precipitation regimes for terrestrial ecosystems. Bioscience 58, 811–821.

Li, F.R., Kang, L.F., Zhang, H., Zhao, L.Y., Shirato, Y., Taniyama, I., 2005. Changes in intensity of wind erosion at different stages of degradation development in grasslands of Inner Mongolia, China. J. Arid Environ. 62, 567–585.

Li, L., Vuichard, N., Viovy, N., Ciais, P., Ceschia, E., Jans, W., Wattenbach, M., Béziat, P., Gruenwald, T., Lehuger, S., 2011. Importance of crop varieties and management practices: evaluation of a process-based model for simulating CO2 and H2O fluxes at five European maize (Zea mays L.) sites. Biogeosciences Discussions 8, 2913–2955.

Li, X.R., Jia, X.H., Dong, G.R., 2006. Influence of desertification on vegetation pattern variations in the cold semi-arid grasslands of Qinghai-Tibet Plateau, Northwest China. J. Arid Environ. 64, 505–522.

Liu, J., Diamond, J., 2005. China's environment in a globalizing world. Nature 435, 1179–1186.

Liu, J., Chen, J.M., Cihlar, J., 2003. Mapping evapotranspiration based on remote sensing: an application to Canada's landmass. Water Resour. Res. 39.

Liu, M., Jiang, G., Li, L., Li, Y., Gao, L., Niu, S., 2004. Control of sandstorms in Inner Mongolia, China. Environ. Conserv. 31, 269–273.

Liu, J., Zhang, Z., Xu, X., Kuang, W., Zhou, W., Zhang, S., Li, R., Yan, C., Yu, D., Wu, S., 2010. Spatial patterns and driving forces of land use change in China during the early 21st century. J. Geogr. Sci. 20, 483–494.

Liu, X., Duan, L., Mo, J., Du, E., Shen, J., Lu, X., Zhang, Y., Zhou, X., He, C., Zhang, F., 2011. Nitrogen deposition and its ecological impact in China: an overview. Environ. Pollut. 159, 2251–2264.

Liu, Y., Liu, R., Chen, J.M., 2012. Retrospective retrieval of long-term consistent global leaf area index (1981–2011) from combined AVHRR and MODIS data. J. Geophys. Res. Biogeosci. 117, G04003.

Liu, Y., Ju, W., He, H., Wang, S., Sun, R., Zhang, Y., 2013. Changes of net primary productivity in China during recent 11 years detected using an ecological model driven by MODIS data. Front. Earth Sci. 7, 112–127.

Lu, Y., Zhuang, Q., Zhou, G., Sirin, A., Melillo, J., Kicklighter, D., 2009. Possible decline of the carbon sink in the Mongolian Plateau during the 21st century. Environ. Res. Lett. 4, 045023.

Luo, Y., Gerten, D., Le Maire, G., Parton, W.J., Weng, E., Zhou, X., Keough, C., Beier, C., Ciais, P., Cramer, W., 2008. Modeled interactive effects of precipitation, temperature, and $[CO_2]$ on ecosystem carbon and water dynamics in different climatic zones. Glob. Chang. Biol. 14, 1986–1999.

Matsushita, B., Tamura, M., 2002. Integrating remotely sensed data with an ecosystem model to estimate net primary productivity in East Asia. Remote Sens. Environ. 81, 58–66.

McMichael, A.J., Powles, J.W., Butler, C.D., Uauy, R., 2007. Food, livestock production, energy, climate change, and health. Lancet 370, 1253–1263.

Melillo, J.M., Steudler, P.A., Aber, J.D., Newkirk, K., Lux, H., Bowles, F.P., Catricala, C., Magill, A., Ahrens, T., Morrisseau, S., 2002. Soil warming and carbon-cycle feedbacks to the climate system. Science 298, 2173–2176.

Mitchell, S.W., Csillag, F., 2001. Assessing the stability and uncertainty of predicted vegetation growth under climatic variability: northern mixed grass prairie. Ecol. Model. 139, 101–121.

Mu, Q., Zhao, M., Running, S.W., Liu, M., Tian, H., 2008. Contribution of increasing CO_2 and climate change to the carbon cycle in China's ecosystems. J. Geophys. Res. Biogeosci. 2005–2012, 113.

Mu, S.J., Zhou, S.X., Chen, Y.Z., Li, J.L., Ju, W.M., Odeh, I.O.A., 2013. Assessing the impact of restoration-induced land conversion and management alternatives on net primary productivity in Inner Mongolian grassland, China. Glob. Planet. Chang. 108, 29–41.

Ni, J., 2000. Net primary production, carbon storage and climate change in Chinese biomes. Nord. J. Bot. 20, 415–426.

Ni, J., 2002. Carbon storage in grasslands of China. J. Arid Environ. 50, 205–218.

Ni, J., 2003. Plant functional types and climate along a precipitation gradient in temperate grasslands, northeast China and southeast Mongolia. J. Arid Environ. 53, 501–516.

Ni, J., 2004a. Estimating net primary productivity of grasslands from field biomass measurements in temperate northern China. Plant Ecol. 174, 217–234.
Ni, J., 2004b. Forage yield-based carbon storage in grasslands of China. Clim. Chang. 67, 237–246.
Parmesan, C., 2007. Influences of species, latitudes and methodologies on estimates of phenological response to global warming. Glob. Chang. Biol. 13, 1860–1872.
Pärtel, M., Helm, A., Reitalu, T., Liira, J., Zobel, M., 2007. Grassland diversity related to the Late Iron Age human population density. J. Ecol. 95, 574–582.
Pei, S., Fu, H., Wan, C., 2008. Changes in soil properties and vegetation following exclosure and grazing in degraded Alxa desert steppe of Inner Mongolia, China. Agric. Ecosyst. Environ. 124, 33–39.
Peng, S., Piao, S., Wang, T., Sun, J., Shen, Z., 2009. Temperature sensitivity of soil respiration in different ecosystems in China. Soil Biol. Biochem. 41, 1008–1014.
Piao, S., Fang, J., Zhou, L., Guo, Q., Henderson, M., Ji, W., Li, Y., Tao, S., 2003. Interannual variations of monthly and seasonal normalized difference vegetation index (NDVI) in China from 1982 to 1999. J. Geophys. Res. Atmos. 1984–2012, 108.
Piao, S., Fang, J., Zhou, L., Ciais, P., Zhu, B., 2006a. Variations in satellite-derived phenology in China's temperate vegetation. Glob. Chang. Biol. 12, 672–685.
Piao, S., Friedlingstein, P., Ciais, P., Zhou, L., Chen, A., 2006b. Effect of climate and CO_2 changes on the greening of the Northern Hemisphere over the past two decades. Geophys. Res. Lett. 33.
Piao, S., Mohammat, A., Fang, J., Cai, Q., Feng, J., 2006c. NDVI-based increase in growth of temperate grasslands and its responses to climate changes in China. Glob. Environ. Chang. 16, 340–348.
Piao, S., Fang, J., Zhou, L., Tan, K., Tao, S., 2007. Changes in biomass carbon stocks in China's grasslands between 1982 and 1999. Glob. Biogeochem. Cycles 21.
Piao, S., Ito, A., Li, S., Huang, Y., Ciais, P., Wang, X., Peng, S., Nan, H., Zhao, C., Ahlström, A., 2012a. The carbon budget of terrestrial ecosystems in East Asia over the last two decades. Biogeosciences 9, 3571–3586.
Piao, S., Tan, K., Nan, H., Ciais, P., Fang, J., Wang, T., Vuichard, N., Zhu, B., 2012b. Impacts of climate and CO2 changes on the vegetation growth and carbon balance of Qinghai–Tibetan grasslands over the past five decades. Glob. Planet. Chang. 98–99, 73–80.
Porporato, A., D'odorico, P., Laio, F., Rodriguez-Iturbe, I., 2003. Hydrologic controls on soil carbon and nitrogen cycles. I. Modeling scheme. Adv. Water Resour. 26, 45–58.
Potter, C.S., Randerson, J.T., Field, C.B., Matson, P.A., Vitousek, P.M., Mooney, H.A., Klooster, S.A., 1993. Terrestrial ecosystem production: a process model based on global satellite and surface data. Glob. Biogeochem. Cycles 7, 811–841.
Schapendonk, A.H.C.M., Stol, W., van Kraalingen, D.W.G., Bouman, B.A.M., 1998. LINGRA, a sink/source model to simulate grassland productivity in Europe. European Journal of Agronomy 9, 87–100.
Schimmelpfennig, S., Müller, C., Grünhage, L., Koch, C., Kammann, C., 2014. Biochar, hydrochar and uncarbonized feedstock application to permanent grassland—Effects on greenhouse gas emissions and plant growth. Agric. Ecosyst. Environ. 191, 39–52.
Scurlock, J., Hall, D., 1998. The global carbon sink: a grassland perspective. Glob. Chang. Biol. 4, 229–233.
Shen, M., Tang, Y., Chen, J., Zhu, X., Zheng, Y., 2011. Influences of temperature and precipitation before the growing season on spring phenology in grasslands of the central and eastern Qinghai-Tibetan Plateau. Agric. For. Meteorol. 151, 1711–1722.
Sitch, S., Friedlingstein, P., Gruber, N., Jones, S.D., Murray-Tortarolo, G., Ahlström, A., Doney, S.C., Graven, H., Heinze, C., Huntingford, C., 2013. Trends and drivers of regional sources and sinks of carbon dioxide over the past two decades. Biogeosci. Discuss. 10, 20113–20177.
Stephens, S.L., Burrows, N., Buyantuyev, A., Gray, R.W., Keane, R.E., Kubian, R., Liu, S.R., Seijo, F., Shu, L.F., Tolhurst, K.G., van Wagtendonk, J.W., 2014. Temperate and boreal forest mega-fires: characteristics and challenges. Front. Ecol. Environ. 12, 115–122.
Sui, X., Zhou, G., 2013. Carbon dynamics of temperate grassland ecosystems in China from 1951 to 2007: an analysis with a process-based biogeochemistry model. Environ. Earth Sci. 68, 521–533.
Sui, X., Zhou, G., Zhuang, Q., 2013. Sensitivity of carbon budget to historical climate variability and atmospheric CO_2 concentration in temperate grassland ecosystems in China. Clim. Chang. 117, 259–272.
Wang, X., Lu, C., Fang, J., Shen, Y., 2007. Implications for development of grain-for-green policy based on cropland suitability evaluation in desertification-affected north China. Land Use Policy 24, 417–424.
Wang, S., Wilkes, A., Zhang, Z., Chang, X., Lang, R., Wang, Y., Niu, H., 2011. Management and land use change effects on soil carbon in northern China's grasslands: a synthesis. Agric. Ecosyst. Environ. 142, 329–340.
Wang, L., Zhou, Y., Zhou, W., Wang, S., 2013. Fire danger assessment with remote sensing: a case study in Northern China. Nat. Hazards 65, 819–834.
Wang, T., Lin, X., Peng, S., Cong, N., Piao, S., 2014. Multimodel projections and uncertainties of net ecosystem production in China over the twenty-first century. Chin. Sci. Bull. 59, 4681–4691.
Warren, C., Dreyer, E., Adams, M., 2003. Photosynthesis-Rubisco relationships in foliage of Pinus sylvestris in response to nitrogen supply and the proposed role of Rubisco and amino acids as nitrogen stores. Trees 17, 359–366.
Xia, J., Luo, Y., Wang, Y.P., Weng, E., Hararuk, O., 2012. A semi-analytical solution to accelerate spin-up of a coupled carbon and nitrogen land model to steady state. Geosci. Model Dev. Discuss. 5, 803–836.
Xing, X., Xu, X., Zhang, X., Zhou, C., Song, M., Shao, B., Ouyang, H., 2010. Simulating net primary production of grasslands in northeastern Asia using MODIS data from 2000 to 2005. J. Geogr. Sci. 20, 193–204.
Yang, K., Koike, T., Ishikawa, H., Kim, J., Li, X., Liu, H., Liu, S., Ma, Y., Wang, J., 2008a. Turbulent flux transfer over bare-soil surfaces: characteristics and parameterization. J. Appl. Meteorol. Climatol. 47, 276–290.
Yang, Y., Fang, J., Tang, Y., Ji, C., Zheng, C., He, J., Zhu, B., 2008b. Storage, patterns and controls of soil organic carbon in the Tibetan grasslands. Glob. Chang. Biol. 14, 1592–1599.
Yang, Y., Fang, J., Ma, W., Guo, D., Mohammat, A., 2010. Large-scale pattern of biomass partitioning across China's grasslands. Glob. Ecol. Biogeogr. 19, 268–277.
Zhang, Y., Zhou, G., 2012. Primary simulation on the response of leaf maximum carboxylation rate to multiple environmental factors (in Chinese). Chin. Sci. Bull. 57, 11–12.
Zhang, Q., S.W., Zhao, D., Dai, E., et al., 2013a. Temporal-spatial Changes in Inner Mongolian Grassland Degradation during Past Three Decades. Agricultural Science & Technology 14, 7.
Zhang, N., Zhao, Y.-S., Yu, G.-R., 2009. Simulated annual carbon fluxes of grassland ecosystems in extremely arid conditions. Ecological Research 24, 185–206.
Zhang, F., Ju, W., Shen, S., Wang, S., Yu, G., Han, S., 2013b. How recent climate change influences water use efficiency in East Asia. Theor. Appl. Climatol. 116, 359–370.
Zheng, Z.-M., Yu, G.-R., Fu, Y.-L., Wang, Y.-S., Sun, X.-M., Wang, Y.-H., 2009. Temperature sensitivity of soil respiration is affected by prevailing climatic conditions and soil organic carbon content: a trans-China based case study. Soil Biol. Biochem. 41, 1531–1540.